TLR9-mediated inflammation drives a Ccr2-independent peripheral monocytosis through enhanced extramedullary monocytopoiesis

Lehn K. Weaver[a], Niansheng Chu[a], and Edward M. Behrens[a,1]

[a]Division of Pediatric Rheumatology, Children's Hospital of Philadelphia, Philadelphia, PA 19104

Edited by Virginia Pascual, Baylor Institute for Immunology Research, Dallas, TX, and accepted by Editorial Board Member Ruslan Medzhitov August 1, 2016 (received for review December 15, 2015)

Monocytes are innate immune cells that interact with their environment through the expression of pattern recognition receptors, including Toll-like receptors (TLRs). Both monocytes and TLRs are implicated in driving persistent inflammation in autoimmune diseases. However, cell-intrinsic mechanisms to control inflammation, including TLR tolerance, are thought to limit inflammatory responses in the face of repeated TLR activation, leaving it unclear how chronic TLR-mediated inflammation is maintained in vivo. Herein, we used a well-characterized model of systemic inflammation to determine the mechanisms allowing sustained TLR9 responses to develop in vivo. Monocytes were identified as the main TLR9-responsive cell and accumulated in peripherally inflamed tissues during TLR9-driven inflammation. Intriguingly, canonical mechanisms controlling monocyte production and localization were altered during the systemic inflammatory response, as accumulation of monocytes in the liver and spleen developed in the absence of dramatic increases in bone marrow monocyte progenitors and was independent of chemokine (C-C motif) receptor 2 (Ccr2). Instead, TLR9-driven inflammation induced a Ccr2-independent expansion of functionally enhanced extramedullary myeloid progenitors that correlated with the peripheral accumulation of monocytes in both wild-type and $Ccr2^{-/-}$ mice. Our data implicate inflammation-induced extramedullary monocytopoiesis as a peripheral source of newly produced TLR9 responsive monocytes capable of sustaining chronic TLR9 responses in vivo. These findings help to explain how chronic TLR-mediated inflammation may be perpetuated in autoimmune diseases and increase our understanding of how monocytes are produced and positioned during systemic inflammatory responses.

monocyte | monocytopoiesis | Toll-like receptor

Monocytes originate from myeloid progenitors in the bone marrow and require active signals through chemokine (C-C motif) receptor 2 (Ccr2) to be released into the circulation and scan the body for sites of inflammation (1, 2). Upon activation, monocytes release proinflammatory mediators, phagocytose invading pathogens and tissue debris, and migrate to tissue draining lymph nodes where they initiate adaptive immune responses (1). The inflammatory cascade established downstream of monocyte activation has been implicated in both the control of infectious diseases and the propagation of sterile inflammation, the latter of which occurs in cancer, atherosclerosis, and systemic autoimmune diseases (3–5). Therefore, mechanisms used to alter the production, function, and/or localization of monocytes are attractive therapeutic targets with broad clinical applications.

Monocytes sense inflammatory cues within their environment through the expression of germ-line–encoded receptors, including Toll-like receptors (TLRs) (6). TLRs are the best-characterized membrane-bound family of pattern recognition receptors, which are receptors activated by specific structural motifs present on a wide variety of microbes or by endogenous "danger" signals (6). Activation through TLR9, in particular, has been implicated in initiating and perpetuating chronic inflammatory diseases, such as lupus and rheumatoid arthritis (7). However, it is unclear how chronic TLR stimulation leads to perpetual inflammation, given the well-characterized phenomenon of TLR tolerance, whereby an initial TLR stimulus leads to an ineffective proinflammatory cytokine response following a secondary TLR stimulus (8–10). Therefore, we sought to determine the mechanisms leading to sustained systemic inflammatory responses downstream of repeated TLR9 activation in vivo.

Previous work demonstrated that systemic inflammation develops downstream of repeated TLR9 activation, leading to cytopenias, splenomegaly, hepatitis, and elevated levels of serum cytokines (11). Interestingly, we now demonstrate that monocytes are the main TLR9-responsive cells and accumulate in peripherally inflamed tissues in this model. Unlike canonical monocyte production and positioning, inflammation-induced monocytopoiesis develops in the absence of dramatic increases in bone marrow monocyte progenitor numbers, and peripheral accumulation of monocytes occurs independent of Ccr2. Instead, Ccr2-independent accumulation of extramedullary myeloid progenitors in peripherally inflamed tissues leads to in situ production of monocytes providing a source of cells to perpetuate the TLR9 response. These findings challenge our current understanding of how monocytes accumulate in inflamed tissues and add additional insight into the perpetuation of inflammatory responses downstream of repeated TLR9 activation in vivo, with broad implications for the development of therapeutic interventions for the treatment of autoimmune diseases.

Significance

Monocytes perpetuate inflammation during autoimmune diseases through chronic sensing of Toll-like receptor (TLR) signals. However, individual monocytes down-regulate their capacity to produce inflammation after an initial TLR-activating event. We now show that continuous TLR9 responsiveness in vivo corresponds to an accumulation of monocytes in peripherally inflamed tissues. Intriguingly, the production and positioning of monocytes occurs independent of the bone marrow, the canonical location of monocyte production during normal homeostasis. Instead, increases in peripheral monocyte numbers are dictated by the accumulation of functionally enhanced monocyte-producing cells in peripherally inflamed tissues. These novel insights into monocyte production and positioning during systemic inflammation implicate local production of TLR-responsive monocytes as a key mechanism contributing to systemic inflammation during autoimmunity.

Author contributions: L.K.W. and E.M.B. designed research; L.K.W. and N.C. performed research; L.K.W., N.C., and E.M.B. analyzed data; and L.K.W. and E.M.B. wrote the paper.

The authors declare no conflict of interest.

This article is a PNAS Direct Submission. V.P. is a Guest Editor invited by the Editorial Board.

[1]To whom correspondence should be addressed. Email: behrens@email.chop.edu.

This article contains supporting information online at www.pnas.org/lookup/suppl/doi:10.1073/pnas.1524487113/-/DCSupplemental.

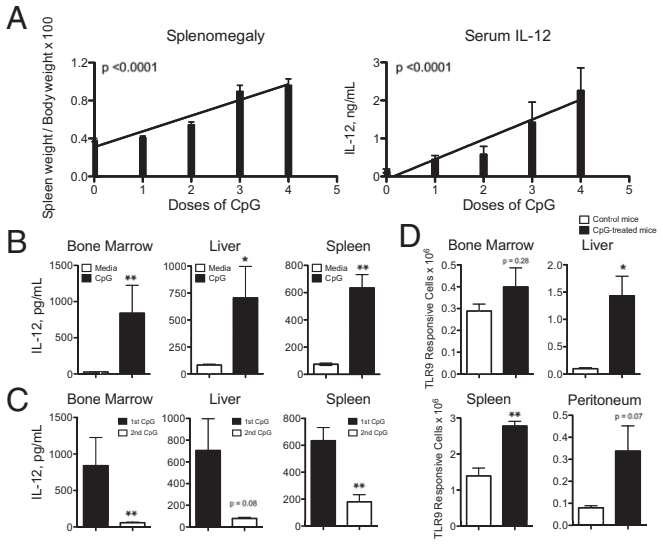

Fig. 1. Systemic inflammation develops downstream of repeated TLR9 activation despite normal TLR9-tolerance mechanisms. C57BL/6 mice were treated with 50 μg of CpG1826 for zero to four doses. (*A*) Twenty-four hours after the last dose of CpG, mice were killed and splenomegaly and serum IL-12 levels were evaluated. Graphs are compiled data from four separate experiments with 14–15 mice per condition and analyzed by linear regression. (*B* and *C*) Bone marrow, liver, and spleen leukocytes were isolated from CpG-treated mice and stimulated with a single dose (*B*) or two consecutive doses of in vitro CpG (*C*). Cell culture supernatants were analyzed for IL-12 and the graphs display representative data of two separate experiments analyzed by Mann–Whitney *u* tests. (*D*) Bone marrow, liver, spleen, and peritoneal leukocytes were isolated from CpG-treated Yet40 (IL-12 reporter) mice and treated with a single dose of ex vivo CpG. YFP expression was measured by flow cytometry and total YFP$^+$ cells were calculated per tissue. The graphs display representative data of three separate experiments analyzed by Mann–Whitney *U* tests. Numbers of significance symbols correspond with the *P* value (i.e., 1 symbol, $P < 0.05$; and 2 symbols, $P < 0.01$).

Results

Systemic Inflammation Downstream of Repeated TLR9 Activation Develops Despite Intact TLR9 Tolerance Mechanisms. An intense area of research into negative regulators of TLR activation has uncovered cell-intrinsic mechanisms used to prevent uncontrolled inflammation from becoming sustained following repeated TLR activation (10). One such mechanism is TLR tolerance, which occurs after TLR-expressing cells are activated by an initial TLR stimulus, rendering them ineffective at generating robust proinflammatory cytokine production upon a secondary TLR stimulus (8–10). We now demonstrate that in vivo treatment of mice with repeated doses of CpG1826, a TLR9 agonist, leads to increasing levels of serum IL-12 and more severe splenomegaly with each additional TLR9 stimulus rather than reduced levels of inflammation expected following canonical TLR tolerance mechanisms (Fig. 1*A*). As IL-12 has previously been shown to be produced downstream of TLR9 activation and is critical for driving systemic immunopathology in vivo (11), we focused our attention on IL-12–producing cells in this model. Cells isolated from CpG-treated mice remain responsive to TLR9 activation, as evidenced by CpG-induced IL-12 production ex vivo (Fig. 1*B*). However, these TLR9 responsive cells undergo TLR9 tolerance normally, as they produce markedly less IL-12 following a secondary CpG stimulus (Fig. 1*C*). Interestingly, using Yet40 (IL-12 reporter) mice to track IL-12–producing cells as a surrogate of TLR9 responsiveness, we demonstrate that TLR9-responsive cells accumulate in multiple peripheral tissues during CpG-induced inflammation (Fig. 1*D*).

Inflammatory Monocytes Are TLR9-Responsive Cells, Accumulate in Peripheral Tissues, and Produce IL-12 in a TLR9 Cell-Intrinsic Manner. To define the cell type(s) responding to repeated TLR9 stimulation, cells were isolated from multiple tissues of Yet40 (IL-12 reporter) mice and stimulated with CpG ex vivo. YFP expression was detected following CpG treatment ex vivo with enhanced percentages of YFP$^+$ cells occurring in tissues isolated from CpG-treated mice (*SI Appendix*, Fig. S1). YFP$^+$ cells expressed both Ly6C and Ccr2 (Fig. 2*A*), known surface markers of inflammatory monocytes (12), implicating monocytes as critical mediators of TLR9-induced inflammation. YFP$^+$ cells isolated from the spleen and peritoneum had less robust expression of Ly6C (Fig. 2*A*), which may be explained by rapid down-regulation of Ly6C upon differentiation of inflammatory monocytes into monocyte-derived dendritic cells (12). This is further supported by the high expression of MHC class II, costimulatory molecules, expression of both CD11b and CD11c, and lack of expression of CD8α on Ly6C^{mid}YFP$^+$ cells (*SI Appendix*, Fig. S2). This phenotype is inconsistent with CD8α$^+$ lymphoid dendritic cells that are classically associated with robust IL-12 production, but rather is consistent with these cells being monocyte-derived dendritic cells. Furthermore, increased numbers of YFP$^+$ cells correlate with the accumulation of inflammatory monocytes in the tissues of CpG-treated mice, as assessed by the percentage and number of Ly6C$^+$Ccr2$^+$ cells in the spleen, liver, peripheral blood, and peritoneum of CpG-treated mice (Fig. 2 *B* and *C* and *SI Appendix*, Fig. S3). Ly6C$^+$Ccr2$^+$ monocytes also express CD115 (*SI Appendix*, Fig. S3), a known inflammatory monocyte marker (1), and express similar levels of TLR9 whether isolated from PBS- or CpG-treated mice (*SI Appendix*, Fig. S4*A*).

We next determined if inflammatory monocytes directly or indirectly produce IL-12 in response to CpG. TLR9-sufficient, but not TLR9-deficient inflammatory monocytes produce IL-12 following CpG stimulation (*SI Appendix*, Fig. S4*B*). Furthermore, TLR9-sufficient, but not TLR9-deficient inflammatory monocytes expressed YFP following CpG treatment in 50:50

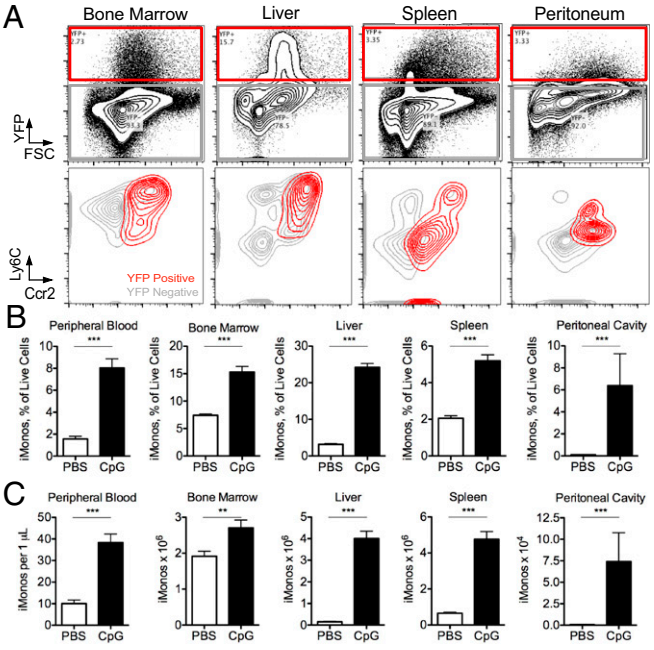

Fig. 2. Inflammatory monocytes are TLR9-responsive cells and accumulate in peripheral tissues following CpG-induced inflammation. Yet40 (IL-12 reporter) mice were treated with or without 50 μg of CpG1826 for four doses and leukocytes were isolated from tissues. (*A*) Cells were stimulated with CpG and the induction of YFP was measured by flow cytometry. YFP$^+$ cells were further characterized by their expression of Ly6C and Ccr2 and plots show representative data of three separate experiments. Percentage (*B*) and total numbers (*C*) of Ly6G$^-$Ly6C$^+$Ccr2$^+$ inflammatory monocytes were enumerated in mice treated with and without repeated TLR9 activation. Graphs show data from seven to eight mice per group and they were analyzed by Mann–Whitney *U* tests. Numbers of significance symbols correspond with the *P* value (i.e., 2 symbols, $P < 0.01$; and 3 symbols, $P < 0.001$).

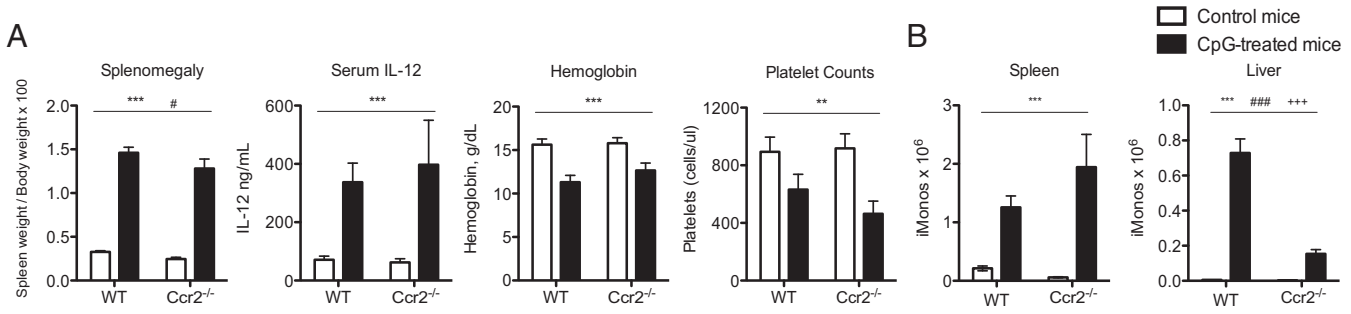

Fig. 3. Peripheral monocytosis occurs independent of Ccr2 correlating with lack of disease protection in $Ccr2^{-/-}$ mice. Wild-type C57BL/6 and $Ccr2^{-/-}$ mice were treated with PBS or 50 μg of CpG1826 for four doses. (*A*) Twenty-four hours after the last dose of CpG, mice were killed and splenomegaly, serum IL-12, anemia, and thrombocytopenia were measured. (*B*) Numbers of spleen and liver $Ly6G^{-}Ly6C^{+}CD115^{+}$ inflammatory monocytes were enumerated from wild-type and $Ccr2^{-/-}$ mice treated with or without CpG. Graphs show data from four mice per group and they were analyzed by two-way ANOVA. (*P* values are denoted as follows: *A* and *B*, *PBS vs. CpG in vivo treatment; #wild-type vs. $Ccr2^{-/-}$; +interaction term.) Numbers of significance symbols correspond with the *P* value (i.e., 1 symbol, $P < 0.05$; 2 symbols, $P < 0.01$; and 3 symbols, $P < 0.001$).

mixed cultures, which correlated to a 50% reduction in IL-12 production in the supernatants of mixed cultures (*SI Appendix*, Fig. S4 *C* and *D*). These data are consistent with TLR9 activating cell-intrinsic production of IL-12 by inflammatory monocytes.

Peripheral Monocytosis Occurs Independent of Ccr2 Correlating with Lack of Disease Protection in $Ccr2^{-/-}$ Mice. Ccr2 is a chemokine receptor that is critically important for mediating the egress of monocytes from the bone marrow (1, 2). Inflammatory monocytes are trapped in the bone marrow of $Ccr2^{-/-}$ mice and are unable to migrate to peripheral sites of inflammation, resulting in defective immune responses and decreased survival in $Ccr2^{-/-}$ mice following infectious challenges (1). As $Ccr2^{+}$ inflammatory monocytes are the main TLR9-responsive cell in CpG-induced inflammation, we predicted that $Ccr2^{-/-}$ mice would be protected from peripheral inflammation during TLR9-induced inflammation. To our surprise, CpG-treated $Ccr2^{-/-}$ mice developed similar levels of splenomegaly, serum IL-12, anemia, and thrombocytopenia compared with wild-type controls (Fig. 3*A*). Although $Ccr2^{-/-}$ mice had defective numbers of peripheral inflammatory monocytes at baseline (*SI Appendix*, Fig. S5*B*), inflammatory monocytes accumulated in the spleens and livers of $Ccr2^{-/-}$ mice following CpG treatment, albeit with reduced hepatic infiltration compared with wild-type mice (Fig. 3*B*). These data were quite surprising, as Ccr2-independent accumulation of monocytes in the spleens and livers of CpG-treated $Ccr2^{-/-}$ mice is in striking contrast with the established dogma that monocytes require an active signal through Ccr2 to egress from the bone marrow. Furthermore, type I/II interferons (IFNs) have been implicated in the expansion of monocytes during systemic inflammation (13, 14). However, neither IL-12 production nor monocyte accumulation was altered in CpG-treated $IFNAR1^{-/-}$ and $IFN\gamma^{-/-}$ mice (*SI Appendix*, Fig. S6).

Peripheral Monocytosis Occurs Independent of a Marked Expansion of Bone Marrow Myeloid Progenitors and Correlates with a Ccr2-Independent Accumulation of Extramedullary Myeloid Progenitors. Under homeostatic conditions, monocytes are produced in the bone marrow from myeloid progenitors (1). To compensate for the increased number of monocytes found in the periphery of CpG-treated mice, we predicted that numbers of bone marrow myeloid progenitors would be increased during TLR9-driven systemic inflammation. However, numbers of bone marrow myeloid progenitors were only mildly affected by CpG-induced inflammation in wild-type and $Ccr2^{-/-}$ mice (Fig. 4*A* and *SI Appendix*, Figs. S7 and S8). We therefore posited that alternative sites of monocytopoiesis might be expanded to compensate for the accumulation of peripheral monocytes seen in CpG-treated mice. A large body of literature has accumulated describing the ability of hematopoietic stem cells (HSCs) to mobilize to the peripheral circulation (15). Evidence for the accumulation of myeloid progenitors in the spleens of mice and humans has also been linked to the propagation of metastatic cancers and atherosclerosis (4, 5). Interestingly, there was a marked expansion of extramedullary myeloid progenitors in the spleen and liver of CpG-treated wild-type and $Ccr2^{-/-}$ mice (Fig. 4 *B* and *C* and *SI Appendix*, Figs. S7 and S8). These data implicate Ccr2-independent extramedullary monocytopoiesis as an in situ source of monocytes during systemic inflammatory responses, which may explain how monocytes accumulate in the periphery of CpG-treated $Ccr2^{-/-}$ mice.

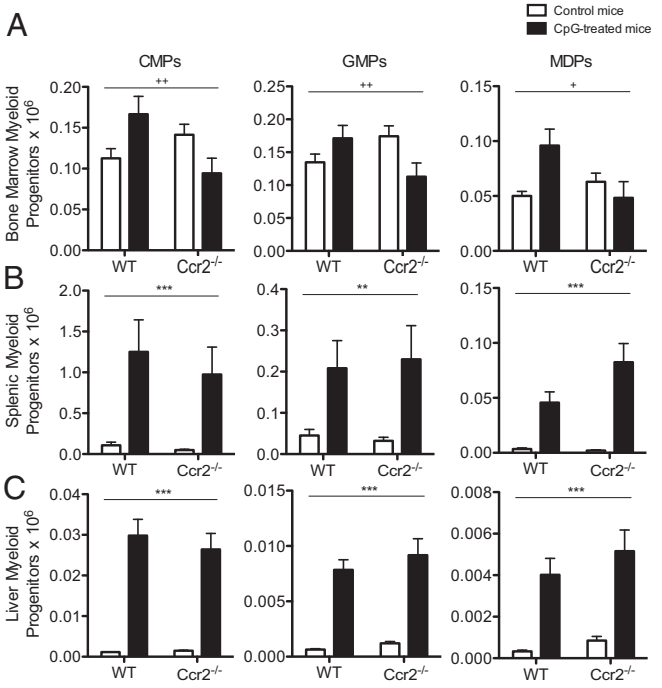

Fig. 4. Peripheral monocytosis occurs independent of an expansion of bone marrow myeloid progenitors and correlates with a Ccr2-independent accumulation of extramedullary myeloid progenitors. Wild-type C57BL/6 and $Ccr2^{-/-}$ mice were treated with PBS or 50 μg of CpG1826 for four doses. Thereafter, the numbers of CMPs, GMPs, and MDPs were enumerated from the bone marrow (*A*), spleen (*B*), and liver (*C*). Graphs display compiled data from three separate experiments with 10–12 mice per group and they were analyzed by two-way ANOVA. (*P* values are denoted as follows: *PBS vs. CpG in vivo treatment; #wild-type vs. $Ccr2^{-/-}$; +interaction term.) Numbers of significance symbols correspond with the *P* value (i.e., 1 symbol, $P < 0.05$; 2 symbols, $P < 0.01$; and 3 symbols, $P < 0.001$).

Myeloid Progenitors Isolated from CpG-Treated Mice Are Bona Fide Producers of TLR9-Responsive Ly6C^{hi} Monocyte-Derived Cells. We performed in vitro monocytopoiesis assays to confirm that our phenotypic characterization of myeloid progenitors identified bona fide myeloid progenitors (*SI Appendix*, Fig. S9*A*). Three distinct populations of progeny, Ly6C^{hi}CD11b^{+}, Ly6C^{mid}CD11b^{+}, and Ly6C^{low}CD11b^{-} cells, were produced by common myeloid progenitor (CMP) and granulocyte–monocyte progenitor (GMP) cultures, whereas monocyte–dendritic cell progenitors (MDPs) produced a single Ly6C^{mid}CD11b^{+} population (Fig. 5 *A* and *B* and *SI Appendix*, Fig. S9 *B* and *C*). Using CMPs isolated from Yet40 (IL-12 reporter) mice, Ly6C^{mid}CD11b^{+} CMP progeny demonstrated inducible YFP expression upon CpG stimulation (Fig. 5 *A* and *B*). Intriguingly, these Ly6C^{mid}CD11b^{+} CMP progeny were not produced early in CMP cultures, but were the dominant cell type that accumulated during long-term CMP cultures (*SI Appendix*, Fig. S10*A*). To determine whether Ly6C^{hi} cells differentiate into Ly6C^{mid} cells during in vitro monocytopoiesis assays, day 10 CMP progeny were sorted into Ly6C^{hi}, Ly6C^{mid}, and CD11b^{-} populations before an additional 14 d of culture. CD11b^{-} cells retained progenitor-like properties and produced all three types of CMP progeny, whereas Ly6C^{hi} and Ly6C^{mid} cells exclusively produced Ly6C^{mid} cells by the end of the culture (*SI Appendix*, Fig. S10 *B* and *C*). These data are consistent with previous data indicating that Ly6C^{hi} monocytes differentiate into Ly6C^{mid} monocyte-derived cells (12). Furthermore, these TLR9-responsive Ly6C^{mid} cells produced during in vitro monocytopoiesis assays expressed high levels of MHC class II, costimulatory markers, CD11b, and CD11c (*SI Appendix*, Figs. S10*D* and S11), which is the same phenotype of the YFP^{+}Ly6C^{mid}Ccr2^{+} population of cells found in CpG-treated mice (*SI Appendix*, Fig. S2). These data confirm that our phenotypic characterization of myeloid progenitors identifies cells capable of producing monocyte-derived cells that are phenotypically and functionally similar to TLR9-responsive cells found in CpG-treated mice.

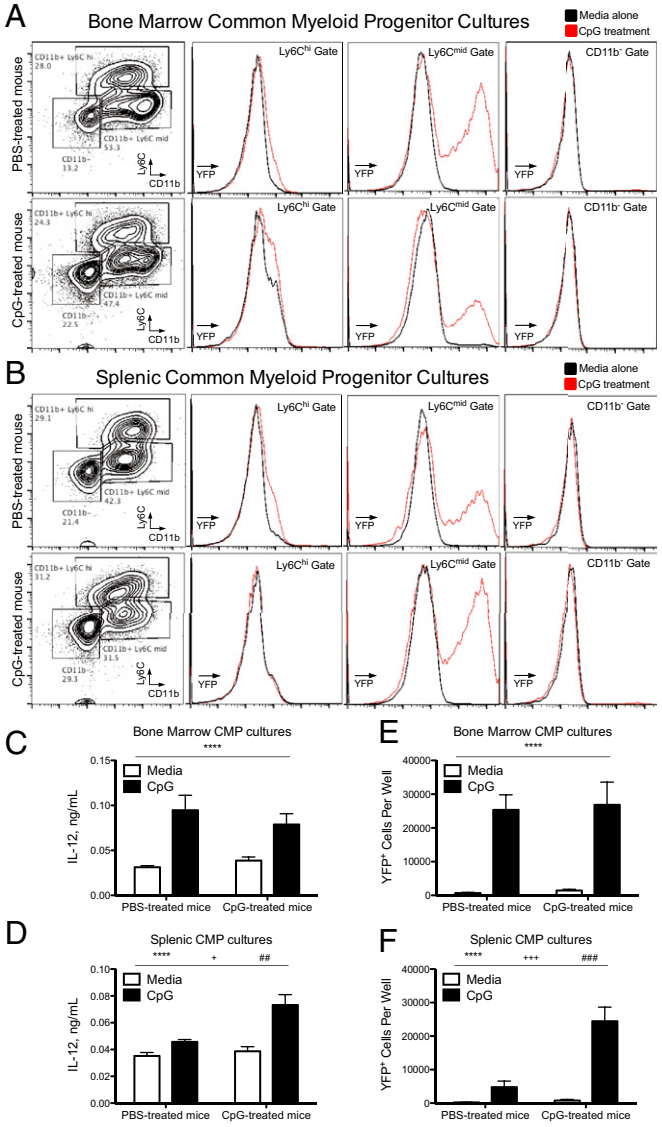

Fig. 5. Extramedullary myeloid progenitors isolated from the bone marrow and spleen are bona fide producers of TLR9-responsive monocytes. CMPs were sorted from Yet40 (IL-12 reporter) mice treated with PBS or 50 μg of CpG1826 for four doses and grown in culture for 2 wk in the presence of myeloid-specific growth factors. The cellular progeny were stained with the myeloid cell markers Ly6C and CD11b with representative flow cytometry plots shown on the *Left* (*A*, bone marrow CMPs; *B*, spleen CMPs). CMP cultures were stimulated with or without CpG during the last 24 h of culture and YFP histograms from the three phenotypically distinct CMP progeny are shown on the *Right* (black line, without CpG; red line, with CpG). CpG-induced IL-12 production from bone marrow (*C*) and spleen (*D*) CMP cultures were analyzed by ELISA. Numbers of YFP^{+} cells from bone marrow (*E*) and spleen (*F*) CMP cultures stimulated with or without CpG were calculated by flow cytometry. Graphs show data compiled from two separate experiments with six to eight mice per group and they were analyzed by two-way ANOVA. (*P* values are denoted as follows: *in vitro treatment with vs. without CpG, $^{\#}$in vivo treatment with PBS vs. CpG, and $^{+}$interaction term.) Numbers of significance symbols correspond with the *P* value (i.e., 1 symbol, $P < 0.05$; 2 symbols, $P < 0.01$; 3 symbols, $P < 0.001$; and 4 symbols, $P < 0.0001$).

Inflammation-Induced Extramedullary Myeloid Progenitors Have Enhanced Monocyte Production Capacity Despite an Erythroid-Megakaryocyte Poised Transcriptional Program. Using our in vitro monocytopoiesis assays, we noticed that inflammation-induced spleen CMP progeny demonstrated enhanced IL-12 production capacity compared with CMP progeny from PBS-treated mice, whereas bone marrow CMP progeny derived from PBS-treated and CpG-treated mice produced similar amounts of IL-12 (Fig. 5 *C* and *D*). This enhanced IL-12 production capacity correlated with an increase in the number of YFP^{+} cells produced in cultures of inflammation-induced spleen CMPs, whereas there was no difference in the number of YFP^{+} cells produced by bone marrow CMPs (Fig. 5 *E* and *F*). Furthermore, the number of Ly6C^{mid}CD11b^{+} progeny produced from spleen CMP and GMP cultures was increased when using progenitors from CpG-treated mice (Fig. 6*B*), albeit the extramedullary CMPs were less efficient than bone marrow CMPs. In contrast, GMPs and MDPs isolated from the bone marrow of PBS- and CpG-treated mice produced similar numbers of the TLR9-responsive Ly6C^{mid}CD11b^{+} progeny (Fig. 6*A*). These data indicate that CpG-induced inflammation leads to enhanced functional output of TLR9-responsive myeloid cells specifically by extramedullary CMPs and GMPs.

We next compared the transcriptomes of CMPs isolated from the bone marrow and spleen of CpG-treated mice. These two populations of cells have dramatically different transcriptomes as assessed by their separation in principal component analysis (PCA) (*SI Appendix*, Fig. S12), unsupervised hierarchical clustering analysis (Fig. 6*C*), and by the large number of differentially expressed genes between these two groups (Fig. 6*D* and *SI Appendix*, Table S1). In contrast, CMPs isolated from the bone marrow of PBS-treated and CpG-treated mice have limited transcriptomic differences, as they cluster closer together in PCA and hierarchical clustering analyses and have very few differentially expressed genes (Fig. 6 *C* and *D* and *SI Appendix*, Fig. S12 and Table S2). Using Ingenuity pathway analysis (IPA), the transcriptional changes between CpG-induced spleen and bone marrow CMPs were predicted to occur through mixed activation and inhibition of monocyte–granulocyte-specific transcription factors, which include relatively increased activity of GFI-1 and reduced function of CEBPα, CEBPε, HOXA9, HOXA7, and SPI-1 in CpG-induced spleen CMPs compared with bone

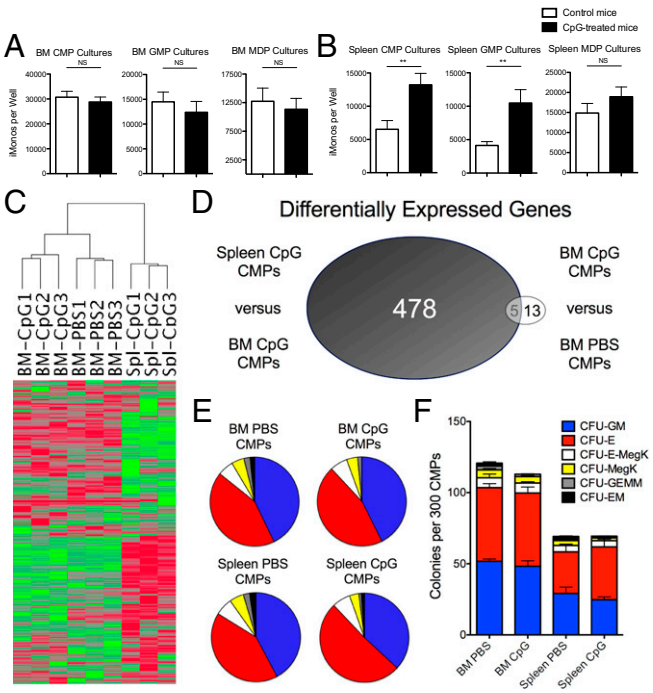

Fig. 6. Inflammation-induced extramedullary CMPs have enhanced monocyte production capacity despite a erythroid-megakaryocyte poised transcriptional program. (*A*) Myeloid progenitors were sorted from mice treated with PBS or 50 μg of CpG1826 for four doses and grown in culture for 2 wk in the presence of myeloid-specific growth factors. The cellular progeny were stained with the myeloid cell markers Ly6C and CD11b. TLR9-responsive monocytes defined as $Ly6C^{mid}CD11b^{+}$ cells from bone marrow (*A*) or spleen (*B*) myeloid progenitor cultures were enumerated by flow cytometry. Graphs show data compiled from three separate experiments with 11–12 mice per group and they were analyzed by Mann–Whitney *u* tests. (*C*) Unsupervised hierarchical clustering analysis is shown for the 3,110 transcripts selected by the expression and variance filters listed in *Materials and Methods* comparing CMPs sorted from the spleen of CpG-treated mice and bone marrow of CpG- and PBS-treated mice ($n = 3$ mice per group). (*D*) Venn diagram shows the number of differentially expressed genes between spleen and bone marrow CMPs from CpG-treated mice versus bone marrow CMPs sorted from PBS- and CpG-treated mice. CMPs were cultured in methylcellulose and the percentages (*E*) and numbers (*F*) of individual types of cfus produced are enumerated ($n = 4$ mice per group for bone marrow CMP samples and $n = 6$–7 mice per group for spleen CMP samples). Numbers of significance symbols correspond with the *P* value (i.e., 2 symbols, $P < 0.01$; and NS, not significant).

marrow CMPs (*SI Appendix*, Table S3). Furthermore, activation of factors involved in erythroid-megakaryocyte differentiation were predicted to have relatively increased function in CpG-induced spleen CMPs compared with bone marrow CMPs including Cdc42, EPO, MKL1, and MKL2 (*SI Appendix*, Table S3). To test the functional outcome of this altered transcriptional program, we performed methylcellulose assays to analyze the capacity of CMPs to produce different types of cfus. To our surprise, the percentage of individual cfus produced by CMPs was not altered by the tissue origin of CMPs or by the CpG-induced inflammatory environment (Fig. 6*E*). However, spleen CMPs had reduced capacity to produce all types of cfus compared with bone marrow CMPs (Fig. 6*F*), indicating that the altered transcriptional program of spleen CMPs reduces their overall cfu capacity rather than skewing the pattern of cfus toward an individual myeloid lineage. Furthermore, our data suggest that CpG-induced spleen CMPs have enhanced monocyte-derived cell production per individual cfu compared with spleen CMPs from control mice, as CpG-induced spleen CMPs produce more monocyte-derived progeny in vitro, despite production of similar numbers of monocyte-specific cfus in methylcellulose assays (Fig. 6 *B* and *F*, respectively). These data support a model whereby TLR9-mediated inflammation induces the accumulation of extramedullary myeloid progenitors that have reduced progenitor capacity compared with bone marrow CMPs, due to an altered transcriptional program. However, inflammation-induced spleen CMPs have enhanced capacity to locally produce TLR9-responsive monocytes compared with baseline spleen CMPs, which contributes to the generation of sustained TLR9-driven inflammatory responses in vivo.

Discussion

Inflammation-induced myelopoiesis is a common endpoint to multiple infectious and inflammatory conditions and has been recognized for decades as a mechanism to provide increased numbers of newly formed innate cells to fuel peripheral inflammatory reactions (16). This "emergency myelopoiesis" has beneficial effects to help control infections, but may also be detrimental in the setting of autoimmune diseases by perpetuating sterile inflammation (17). Herein, we add support to this latter hypothesis by demonstrating that TLR9-mediated sterile inflammation leads to enhanced production and accumulation of TLR9-responsive monocytes. We propose that enhanced monocytopoiesis generates a continuous source of new TLR-responsive monocytes to perpetuate an inflammatory response in the face of cell-intrinsic TLR-tolerance mechanisms. Although TLR tolerance likely dampens inflammatory reactions during acute inflammatory responses (8, 9), continuous production of new TLR-responsive cells through an expansion of monocytopoiesis may perpetuate chronic inflammation in TLR-driven autoimmune diseases. Therefore, understanding the mechanisms leading to inflammation-induced monocytopoiesis could inform future efforts to therapeutically target this pathway for the treatment of sterile inflammatory diseases.

Herein, we begin to unravel the mechanisms driving inflammation-induced monocytopoiesis downstream of repeated TLR9 activation, which is characterized by unique properties compared with monocyte production during normal homeostasis. We first demonstrate the unexpected finding that bone marrow monocytopoiesis is only mildly increased during TLR9-mediated inflammation, despite a large increase in the number of peripheral tissue monocytes. Furthermore, monocytes accumulate in the spleen of CpG-treated $Ccr2^{-/-}$ mice similarly to CpG-treated wild-type mice, implicating a Ccr2-independent mechanism leading to peripheral monocytosis during TLR9-driven systemic inflammation. To resolve these discrepancies with the current dogma of monocyte production and positioning, we demonstrate that myeloid progenitors accumulate in the liver and spleen of CpG-treated mice independent of Ccr2. Despite having a poised erythroid-megakaryocyte transcriptional program, CpG-induced spleen CMPs maintain enhanced capacity to produce TLR9-responsive monocytes compared with baseline spleen CMPs. Inflammation-induced extramedullary monocytopoiesis is not likely an epiphenomenon found only in rodents, as extramedullary myeloid progenitors have been found in patients with multiple autoimmune rheumatic diseases (18, 19). Furthermore, these data may explain why drugs targeting the previously promising therapeutic target, Ccr2, have not been successful in the treatment of autoimmune diseases in the clinic, as our data suggest a Ccr2-independent mechanism allowing monocytes to be produced locally in inflamed tissues during sustained TLR9-mediated inflammatory responses. As human monocytes do not express TLR9, additional work will be needed to translate these intriguing possibilities to the clinic where other inflammatory mediators may coalesce to drive inflammation-induced monocytopoiesis and sustain systemic autoimmune responses.

Our data challenge the current paradigm of how monocytes are produced and positioned during systemic inflammation by implicating Ccr2-independent in situ production of monocytes as a key mechanism contributing to monocyte dynamics during systemic inflammatory responses. Furthermore, this study expands our understanding of TLR biology by providing an explanation for how chronic TLR stimulation can lead to sustained inflammatory responses through the continuous production of new TLR responsive cells in the face of cell-intrinsic TLR-tolerance immunoregulatory

mechanisms. In conclusion, these findings offer new insight into monocyte biology and have practical implications for how TLR responses are propagated in sterile inflammatory conditions.

Materials and Methods

Animals. Six- to 12-wk old mice were used for all experiments. C57BL/6, C57BL/6.SJL, Yet40 (IL-12 p40 reporter), Ccr2$^{-/-}$ RFP, and IFNγ$^{-/-}$ mice were purchased from The Jackson Laboratory. TLR9$^{-/-}$ and IFNAR1$^{-/-}$ mice were maintained in our colony, as previously described (20). TLR9$^{-/-}$ and Yet40 mice were bred together to generate homozygous TLR9$^{-/-}$ Yet40 mice (CD45.2.2). Yet40 and SJL mice were bred together to generate homozygous TLR9$^{+/+}$ SJL Yet40 mice (CD45.1.1). All mice were bred and maintained at the University of Pennsylvania or the Children's Hospital of Philadelphia animal facilities and cared for according to the institutions' animal facility guidelines. All procedures were performed after approval by institutional ethics boards.

Cellular Immunophenotyping. Detailed methods for flow cytometry analyses can be found in *SI Appendix, SI Methods*. Inflammatory monocytes were identified as Ly6G$^-$Ly6C$^+$Ccr2$^+$ or Ly6G$^-$Ly6C$^+$CD115$^+$ cells, as described in figure legends. Myeloid progenitors were identified as CMPs (Lin$^-$c-Kit$^+$CD105$^-$CD16/32^{low}CD115$^-$), GMPs (Lin$^-$c-Kit$^+$CD105$^-$CD16/32^{high}CD115$^-$), MDPs (Lin$^-$c-Kit$^+$CD105$^-$CD115^{high}), or common monocyte progenitors (cMoPs; Lin$^-$c-Kit$^+$CD105$^-$CD115^{high}Ly6C$^+$). The lineage panel included antibodies against B220, CD4, CD5, CD8a, CD11b, CD11c, CD90.2, DX5, Gr-1 (Ly6C/Ly6G), NK1.1, and Ter119, except for identification of cMoPs where Ly-6G was used instead of GR-1.

TLR9-Mediated Model of Systemic Inflammation and Tissue Processing. The class B CpG1826 oligonucleotide was synthesized by Integrated DNA Technologies. Mice were injected with PBS or 50 μg of CpG1826 intraperitoneally every other day for zero to four doses. Mice were killed 24 h after the last injection and organs were harvested for analysis. Organs were processed by filtering over a 70-μm strainer to obtain single cells before RBC lysis and counting. Organ-specific details of cell isolation are provided in *SI Appendix, SI Methods*.

Identification of TLR9-Responsive Cells. Leukocytes were harvested from multiple tissues and cultured in vitro as described in *SI Appendix, SI Methods*. Cells were treated with 10 μg/mL CpG1826 for 20 h before harvesting cell culture supernatants for IL-12 detection by ELISA and analysis of YFP expression by flow cytometry. For TLR9-tolerance assays, leukocytes were treated with 10 μg/mL CpG1826 for 20 h. A second TLR9 stimulus with 10 μg/mL CpG1826 was immediately performed after removal of the supernatant following the first stimulation for an additional 20-h stimulation.

In Vitro Hematopoiesis Assay.
Monocytopoiesis assays. Sorted myeloid progenitors (100-2000 cells per well of a 24-well plate) were cultured in MEM-α media (Gibco) supplemented with 20% heat-inactivated FBS and penicillin–streptomycin–L-glutamine. GM-CSF, M-CSF, IL-3, and stem cell factor were obtained from Peprotech to supplement these cultures. At the end of culture, myeloid progenitor progeny were analyzed for myeloid surface markers and total cell counts by flow cytometry or stimulated with 10 μg/mL CpG1826 for 20 h to analyze YFP expression and IL-12 production by ELISA.
Methylcellulose assays. CMPs were sorted from the bone marrow and spleen of PBS- and CpG-treated mice. A total of 300 CMPs were cultured in MethoCult (Stemcell Technologies). On day 10–11 of culture, cfus were enumerated.

RNA Microarray. CMPs were sorted into lysis buffer for RNA purification, amplification, and hybridization to the mouse Affymetrix ST 2.0 GeneChip. The microarray dataset was filtered on probesets with annotations of gene symbols in the Refseq and ENSEMBL databases, for a total of 10,527 genes used for PCA analysis. Further filtering using a minimum $\log_2$ intensity value of 5 and a minimum $\log_2$ difference between row values of 0.5 resulted in 3,110 transcripts used for unsupervised hierarchical clustering analysis. Differentially expressed genes (DEGs) between CMPs were determined with a false-discovery rate cutoff of 0.1 by the Benjamini–Hochberg procedure. IPA upstream analysis of DEGs was used to predict regulators of the transcriptional changes between spleen and bone marrow CMPs isolated from CpG-treated mice using a P value of <0.0001 and an absolute value Z score of ≥ 2. Further details are provided in *SI Appendix, SI Methods*.

Statistical Analyses. Linear regression was used to model the relationship between the number of doses of CpG and the development of splenomegaly and serum IL-12. Mann–Whitney u tests were performed for all single comparisons. One-way ANOVA was performed with Bonferroni posttest analysis to analyze data with multiple single comparisons. Two-way ANOVAs were performed to simultaneously analyze the interaction between two independent variables on a dependent variable. Numbers of significance symbols correspond with the P value, as follows (i.e., 1 symbol $P < 0.05$; 2 symbols $P < 0.01$; 3 symbols $P < 0.001$; 4 symbols $P < 0.0001$; NS, not significant).

ACKNOWLEDGMENTS. The authors thank Hamid Bassiri, Martha Jordan, Taku Kambayashi, Paula Oliver, Gary Koretzky, and members of their associated laboratories for support and helpful discussions; and the flow cytometry core at the University of Pennsylvania for technical help with cell sorting. E.M.B. was funded by the National Heart, Lung, and Blood Institute Grant R01HL112836 and a Howard Hughes Medical Institute early career investigator award. L.K.W. was funded by a Rheumatology Research Foundation scientist development award and NIH Training Grants AR007442-26A1 and HD043021-09.

1. Shi C, Pamer EG (2011) Monocyte recruitment during infection and inflammation. *Nat Rev Immunol* 11(11):762–774.
2. Kuziel WA, et al. (1997) Severe reduction in leukocyte adhesion and monocyte extravasation in mice deficient in CC chemokine receptor 2. *Proc Natl Acad Sci USA* 94(22):12053–12058.
3. Getts DR, et al. (2014) Therapeutic inflammatory monocyte modulation using immune-modifying microparticles. *Sci Transl Med* 6(219):219ra7.
4. Swirski FK, et al. (2006) Monocyte accumulation in mouse atherogenesis is progressive and proportional to extent of disease. *Proc Natl Acad Sci USA* 103(27):10340–10345.
5. Pittet MJ, Swirski FK (2011) Monocytes link atherosclerosis and cancer. *Eur J Immunol* 41(9):2519–2522.
6. Jiménez-Dalmaroni MJ, Gerswhin ME, Adamopoulos IE (2016) The critical role of toll-like receptors—From microbial recognition to autoimmunity: A comprehensive review. *Autoimmun Rev* 15(1):1–8.
7. Ewald SE, Barton GM (2011) Nucleic acid sensing Toll-like receptors in autoimmunity. *Curr Opin Immunol* 23(1):3–9.
8. Foster SL, Hargreaves DC, Medzhitov R (2007) Gene-specific control of inflammation by TLR-induced chromatin modifications. *Nature* 447(7147):972–978.
9. López-Collazo E, del Fresno C (2013) Pathophysiology of endotoxin tolerance: Mechanisms and clinical consequences. *Crit Care* 17(6):242.
10. Liew FY, Xu D, Brint EK, O'Neill LA (2005) Negative regulation of Toll-like receptor-mediated immune responses. *Nat Rev Immunol* 5(6):446–458.
11. Behrens EM, et al. (2011) Repeated TLR9 stimulation results in macrophage activation syndrome-like disease in mice. *J Clin Invest* 121(6):2264–2277.
12. Cheong C, et al. (2010) Microbial stimulation fully differentiates monocytes to DC-SIGN/CD209(+) dendritic cells for immune T cell areas. *Cell* 143(3):416–429.
13. Buechler MB, Teal TH, Elkon KB, Hamerman JA (2013) Cutting edge: Type I IFN drives emergency myelopoiesis and peripheral myeloid expansion during chronic TLR7 signaling. *J Immunol* 190(3):886–891.
14. de Bruin AM, et al. (2012) IFNγ induces monopoiesis and inhibits neutrophil development during inflammation. *Blood* 119(6):1543–1554.
15. Motabi IH, DiPersio JF (2012) Advances in stem cell mobilization. *Blood Rev* 26(6): 267–278.
16. Takizawa H, Boettcher S, Manz MG (2012) Demand-adapted regulation of early hematopoiesis in infection and inflammation. *Blood* 119(13):2991–3002.
17. Hamilton JA (2008) Colony-stimulating factors in inflammation and autoimmunity. *Nat Rev Immunol* 8(7):533–544.
18. Horie S, et al. (1997) Detection of large macrophage colony forming cells in the peripheral blood of patients with rheumatoid arthritis. *J Rheumatol* 24(8):1517–1521.
19. López-Karpovitch X, Cardiel M, Cardenas R, Piedras J, Alarcón-Segovia D (1989) Circulating colony-forming units of granulocytes and monocytes/macrophages in systemic lupus erythematosus. *Clin Exp Immunol* 77(1):43–46.
20. Baratono SR, Chu N, Richman LP, Behrens EM (2015) Toll-like receptor 9 and interferon-γ receptor signaling suppress the B-cell fate of uncommitted progenitors in mice. *Eur J Immunol* 45(5):1313–1325.